Dyes and Pigments **14** (1990) 165–189

Azo-Hydrazone Tautomerism of an *o,o'*-Dihydroxy Azo Dye—A Spectroscopic Study

Bing R. Hsieh

Xerox Corporation, Webster Research Center, Webster, New York 14580, USA

Denis Désilets & Peter M. Kazmaier

Xerox Research Centre of Canada, Mississauga, Ontario, Canada L5K 2L1

(Received 18 October 1989; accepted 15 November 1989)

ABSTRACT

*The aggregation behavior and tautomerism of an o,o'-dihydroxy azo dye, namely 4-(3',5'-dinitro-2'-hydroxyphenylazo)-3-hydroxy-2-naphthanilide (**A**) and its ionized counterpart **B** were studied by UV-VIS spectroscopy. The dyes showed similar absorption behaviors in all the solvents investigated and in the solid state. Concentration dependent spectroscopic changes with the formation of isobestic points were observed in DMF and DMSO, indicating dimer–monomer equilibria. Deconvolution of representative absorption profiles of **A** and **B** gave four Gaussian peaks at about 450, 550, 580 and 620 nm. Whilst these peak positions remained relatively constant, the peak areas varied with respect to the change of the dye concentration. By comparing the deconvoluted absorption maxima to those estimated by PPP-CI calculations, the conclusion was reached that the spectroscopic changes were due to a shift of the hydrazone–azo equilibria caused by the shifting of the dimer–monomer equilibrium, i.e., the aggregated dye molecules exist*

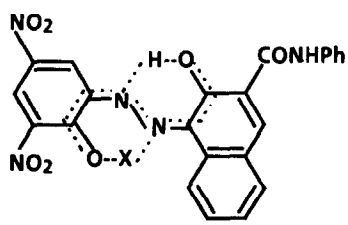

A X = H
B X = Na

Dyes and Pigments 0143-7208/90/$03·50

mainly in hydrazone form while the monomeric dye molecules prefer the azo form. A theory is presented to explain the observation that the tautomeric mixtures of **A** *and* **B** *were closely related, that is, they had similar UV-VIS behavior and they showed almost identical IR, Raman and NMR spectra. An intermediate which involves a completely delocalized structure shown above is proposed. This structure may be regarded as the transitional species that bridges the three possible tautomers, namely azo, naphthoquinone–hydrazone and benzoquinone–hydrazone of* **A** *or* **B**. *The X (X = H or Na) may undergo rapid intramolecular transfer between the azo nitrogens and the phenoxy oxygens and the tautomers of* **A** *may be as ionic as the tautomers of* **B**.

1 INTRODUCTION

The azo-hydrazone tautomerism of *o*-hydroxy azo dyes, such as the derivatives of 1-phenylazo-2-naphthol (Scheme 1), has been extensively studied by various spectroscopic methods and theoretical treatments. Many important factors governing the equilibrium between these two tautomers have been established.[1-6] A recent publication has summarized much of the

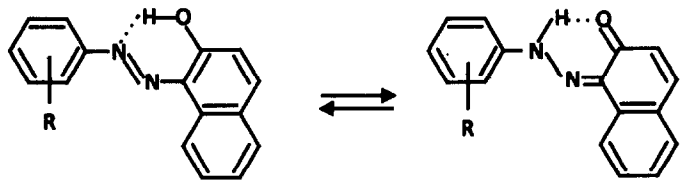

Scheme 1

up-to-date knowledge about the subject and also made a very important conclusion that the phenoxy proton underwent rapid intramolecular switching between nitrogen and oxygen atoms at a rate of about $2 \times 10^3\ s^{-1}$ in solution as well as in the solid state.[7]

The tautomerism of *o,o'*-dihydroxy azo compounds, on the other hand, is not well understood and relevant publications are few.[8-12] Yagi studied the tautomerism of 1-(2'-hydroxyphenylazo)-2-naphthol in neutral and alkaline aqueous methanol solutions by UV spectroscopy.[8] The author suggested that the absorption maxima (λ_{max}) at 422 and 508 nm (with an inflection point at 539 nm) in 50/50 water/methanol were due to tautomers **I** and **II** (Scheme 2). In 0·01 or 0·1 N NaOH/methanol, the dye showed λ_{max} at about 390 and 575 nm. These were attributed to **III** and **IV** respectively by Yagi. The λ_{max} at 446 nm and the one at 527 nm (with an inflection point at 608 nm) observed in 0·5 N KOH/methanol were attributed to tautomers **V** and **VI** respectively. The evidence for this assignment was not compelling and apparently the influence of dye aggregation on the overall absorption

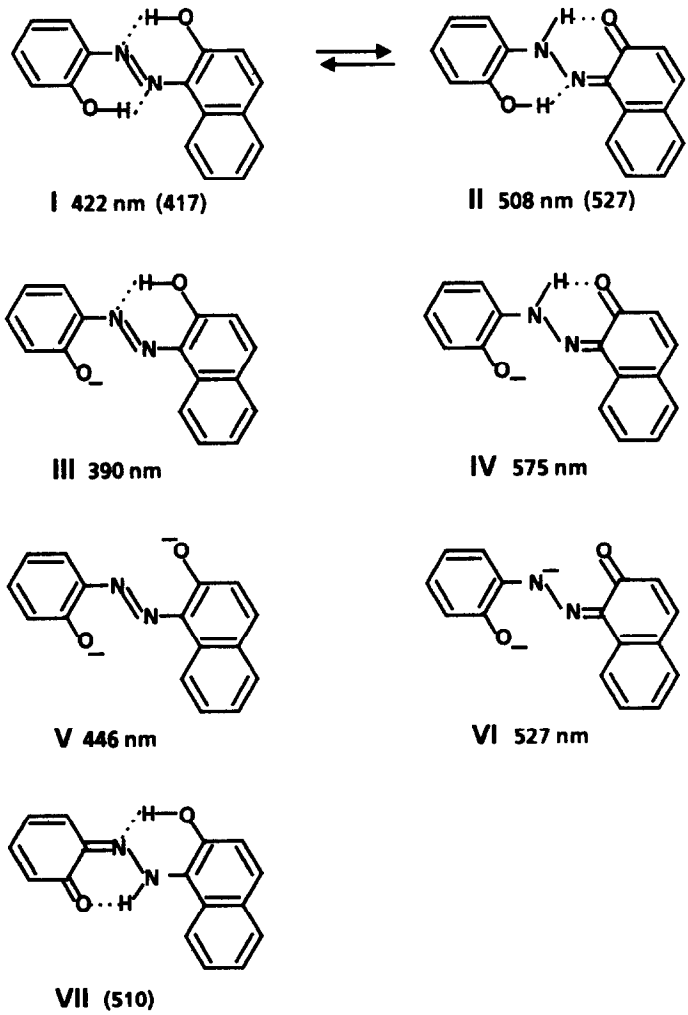

Scheme 2

spectra were neglected even though aggregation is known to have a significant impact on the absorption spectra.[13]

A different interpretation of Yagi's results was later described by Pilipenko & Savranskii.[9] In addition to **I** and **II**, they proposed a new tautomer, **VII**, for the dye at its neutral state. These authors obtained the respective theoretical λ_{max} of 417, 527, and 510 nm for the tautomers by Pariser–Parr–Pople (PPP) calculations. Their results could interpret the observed λ_{max} very well as follows: the absorption bands of **VII** and **II** may overlap and give rise to the 508 nm band with an inflection point at 539 nm. Furthermore, the Russian workers obtained a calculated λ_{max} of 564 nm for structure **VIII** (Scheme 3) and suggested that it was responsible for the

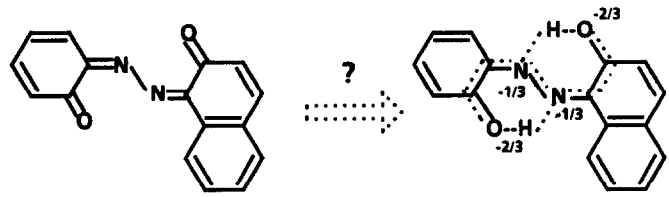

VIII (564) **IX**

Scheme 3

bathochromic shift in the alkaline solutions observed by Yagi. They mentioned that this neutral structure was to represent the dye in a di-ionized state. This is very confusing and could be the reason why the discussion of **VIII** has been avoided by recent researchers, even though they have accepted tautomers **I**, **II** and **VII**.[6,11,12,14] Based on the description by the Russian workers, we speculated that structure **IX** was what they had in mind. This structure may be regarded as di-anionic with two negative charges distributed among two azo nitrogens and two phenoxy oxygens. And, protons are the corresponding counter ions. However, as a whole, **IX** is neutral. The partial charge given for each atom is an average over three possible di-anionic forms (see Section 3).

We studied the tautomerism of another *o,o'*-dihydroxy azo dye, namely 4-(3',5'-dinitro-2'-hydroxyphenylazo)-3-hydroxy-2-naphthanilide (**A**, as shown in Scheme 4) and its ionized counterpart **B**, which contains an ionized phenoxy group (see Section 2 for details). UV-VIS results, in solution (DMF, DMSO and acetone) and in solid state (KBr), are reported in this paper. We found that the tautomerism of **A** and **B** was affected by the state of dye aggregation which in turn is affected by the solvent. Selected UV-VIS spectra

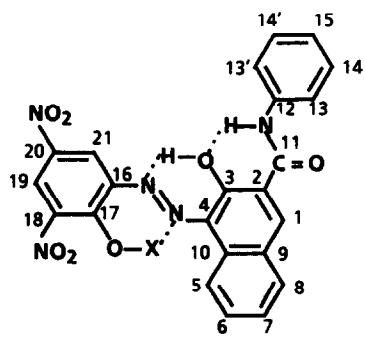

A X = H
B = Na

Scheme 4

were deconvoluted into individual Gaussian peaks which were then assigned to the corresponding tautomers based on the results of PPP-CI calculations. The results of FT-IR, Raman, and NMR are also included to provide additional structural information.

2 EXPERIMENTAL

2.1 Instrumentation

IR spectra (in KBr) were recorded on a Perkin-Elmer 1750 Fourier transform spectrometer. Raman measurements were performed with the 4880 Å line of an argon-ion laser at power of 40–120 mW. A spex triple-monochromator system was used to reduce the level of scattered light. The spectrometer splits were set for a resolution of 4 cm^{-1}. The sample (in KBr) was kept at room temperature during measurement with scanning range from 900 to 2000 cm^{-1}. Since azo compounds absorb in the FT-IR laser region, care must be taken to avoid photofading during data acquisition. The azo compounds showed reproducible spectra in the first two scans. However, some decomposition was detected afterwards. ^{13}C NMR spectra (in DMSO or in the solid state) were recorded on a Bruker CXP spectrometer operating at 50·3 MHz in a superconducting magnet system (Cryomegnet Systems Inc). Proton-enhanced cross polarization used 3–6 ms contact times, high power (H1 = 12 G) proton decoupling and recycle times of 1–3 s. Magic angle spinning (4–4·5 KHz) was performed in a Doty Scientific probe with about 100 mg of each sample packed into 6 mm o.d. sapphire rotors. The TOSS technique for sidebands suppression was used for all measurements. Typically, 256–10 000 scans were averaged for each spectrum. ^{1}H and ^{1}H–^{13}C 2D NMR spectrometry was performed on a Bruker AM-360 system equipped with 5 mm QNP probe. Solutions prepared in DMSO-d_6 at about 10 wt% for heteronuclear shift-correlated studies[15] and about 1 wt% or less for simple acquisitions. UV-VIS spectra were recorded on a Hewlett-Packard 8451A diode array spectrophotometer. UV-VIS spectra of **A** and **B** were measured in acetone, DMF or DMSO at different concentrations. Typically, a solution of **A** or **B** (2·5–3·1 mg) in 100 ml of solvent was initially prepared in an 100 ml volumetric flask. The solution (10 ml) was transferred into a vial and mixed with 20 ml of the pure solvent to give the second solution. This was used to prepare further diluted solutions by the same procedure. To obtain consistent and reproducible results, the same cuvette was used for a particular set of measurements and it was rinsed with acetone and then air dried before use. For solid state UV-VIS measurements, about 1 mg of **A** or **B** was mixed with 500 mg of KBr in a

TABLE 1

Calculated Absorption Maxima and Oscillator Strength for Possible Tautomers

Tautomers	λ_{max}	*OS*
N1[a]	482	1·020
	353	0·320
	521	0·959
	389	0·309
N2[a]	376	0·063
	345	0·056
	342	0·126
	595	0·988
N3[a]	366	0·258
	341	0·172
	629	0·506
N3′[a]	363	0·054
	345	0·303
	589	0·846
M1[b]	419	0·410
	374	0·002
	349	0·252
	625	1·02
M2[b]	438	0·267
	400	0·043
	371	0·017
	613	0·938
M3[b]	422	0·155
	399	0·164
	368	0·052
	592	0·820
	526	0·300
D1[c]	428	0·069
	379	0·008
	366	0·338
	634	0·614
	625	0·422
D2[c]	470	0·007
	407	0·175
	380	0·341
	598	0·669
	570	0·264
D3[c]	396	0·084
	392	0·003
	363	0·362
	597	0·834
	547	0·281
D[c]	432	0·037
	381	0·001
	369	0·398

[a] See Scheme 5. [b] See Scheme 6. [c] See Scheme 7.

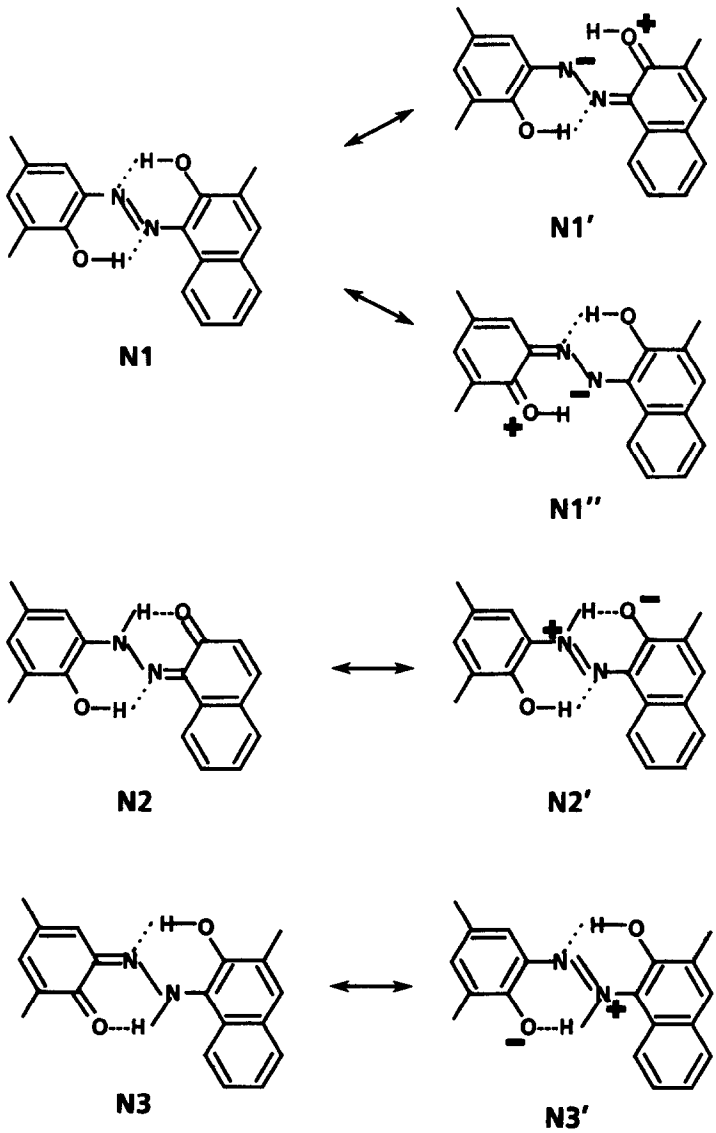

Scheme 5

ball mill. From about 80 mg of the resulting powder, a pellet with 1 cm diameter was prepared. Peak deconvolution of the spectra was performed using a non-linear least squares optimization procedure. PPP calculations with configuration interaction (CI) were done with a PPP-CI program.[16] The calculations assumed planar geometries with hydrogen bonding as shown in Scheme 4. The calculations for the negatively charged intermediates assumed a fully delocalized charge; therefore, they do not account for tight

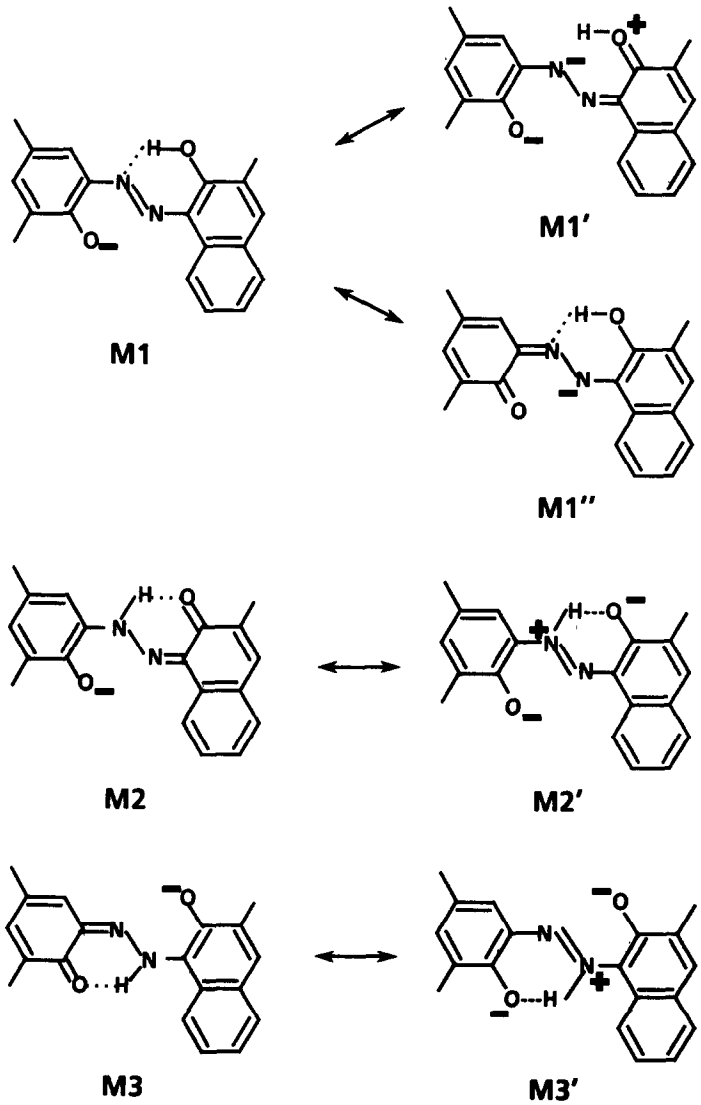

Scheme 6

ion pairs where the charge is more localized. The parameters used for the calculation of **D** (see Scheme 7 and Table 1) were an average of the ones used for **D1**, **D2** and **D3**.

2.2 Materials

Compound **A** was obtained by acid treatment (3% aqueous HCl) of **B**, which was received as a gift from Hodogaya Chemical Co. Ltd, Tokyo, Japan (the

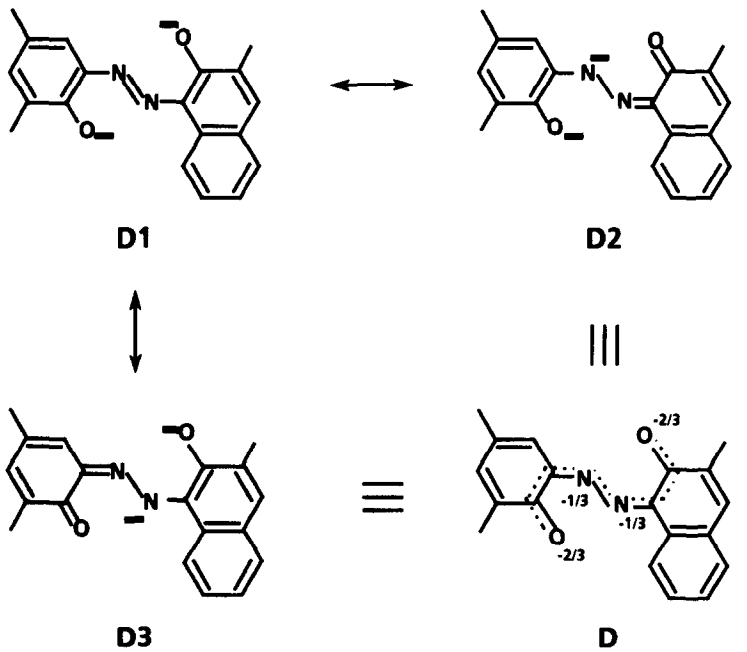

Scheme 7

synthesis of **A** was described in Refs 17 and 18). Compound **A** which was black-purple gave dark greenish solution in DMSO or DMF, whilst the dark greenish **B** gave black-blue DMSO or DMF solutions. Compound **B** gave the following elemental analysis data: C 55·88, H 2·95, N 13·89, Na 5·13. These correspond well with the calculated values for the mono-ionized **A** with chemical formula of $C_{23}H_{14}N_5O_7Na$: C 55·76, H 2·83, N 14·14, Na 4·64. This indicates that **B** is mainly mono-ionized and is in agreement with ^1H NMR result (see Section 3). Compound **A** showed the following analytical data: C 52·26, H 3·63, N 13·37, Na 0·03, corresponding well with the calculated values for $C_{23}H_{15}N_5O_7 . 3H_2O$: C 52·37, H 3·98, N 13·28. DMF and DMSO were purchased from J. T. Baker Chemical Co. and were used as received.

3 RESULTS AND DISCUSSION

3.1 Dye aggregation in solution

The absorption spectra of **A** in DMF and DMSO at different concentrations are shown in Fig. 1(a) and (b) respectively, while those of **B** are shown in Fig. 2(a) and (b). In all cases, hydrazone tautomers had their highest absorption

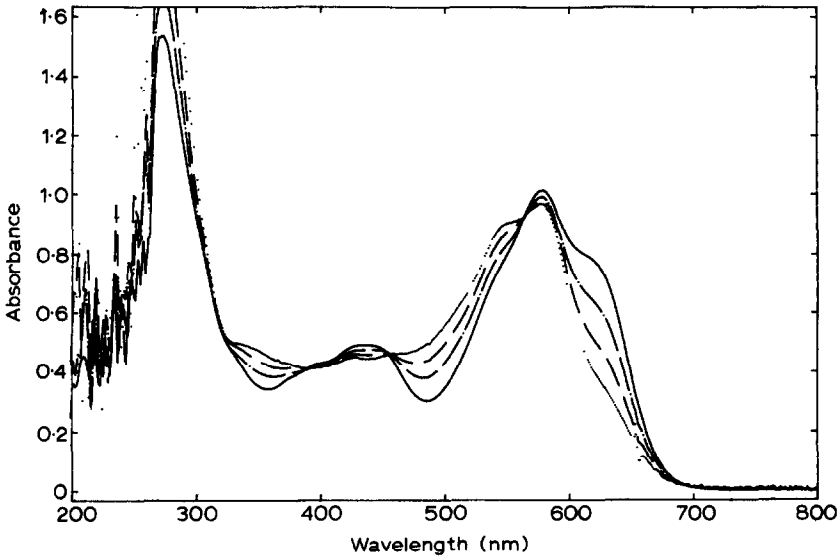

(a)

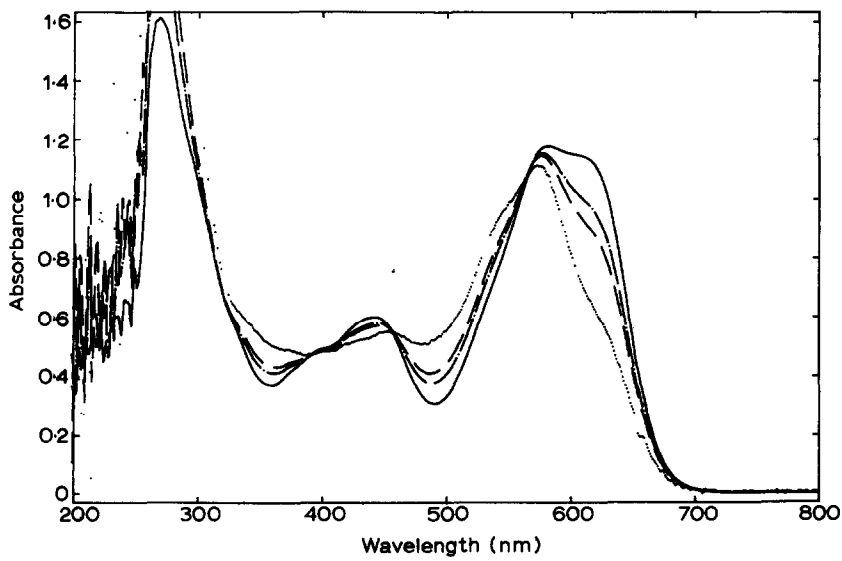

(b)

Fig. 1. (a) The normalized absorption spectra of **A** in DMF at $5{\cdot}29 \times 10^{-6}$ M (——); $1{\cdot}32 \times 10^{-6}$ M (– · –); $6{\cdot}61 \times 10^{-7}$ M (– –); $3{\cdot}30 \times 10^{-7}$ M (· · · · · ·). (b) The normalized absorption spectra of **A** in DMSO at $5{\cdot}29 \times 10^{-6}$ M (——); $1{\cdot}32 \times 10^{-6}$ M (– · –); $6{\cdot}61 \times 10^{-7}$ M (– –); $1{\cdot}65 \times 10^{-7}$ M (· · · · · ·). (The absorbance is given for the spectrum with the highest concentration in each case.)

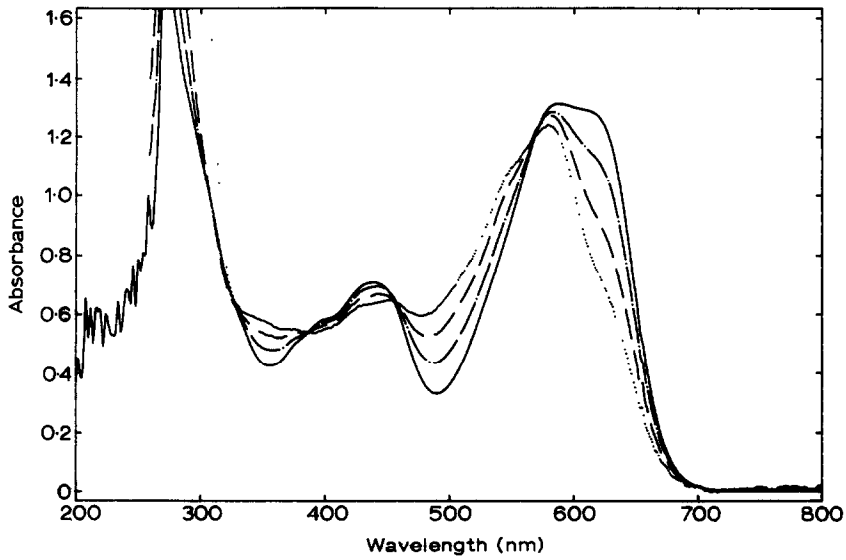

(a)

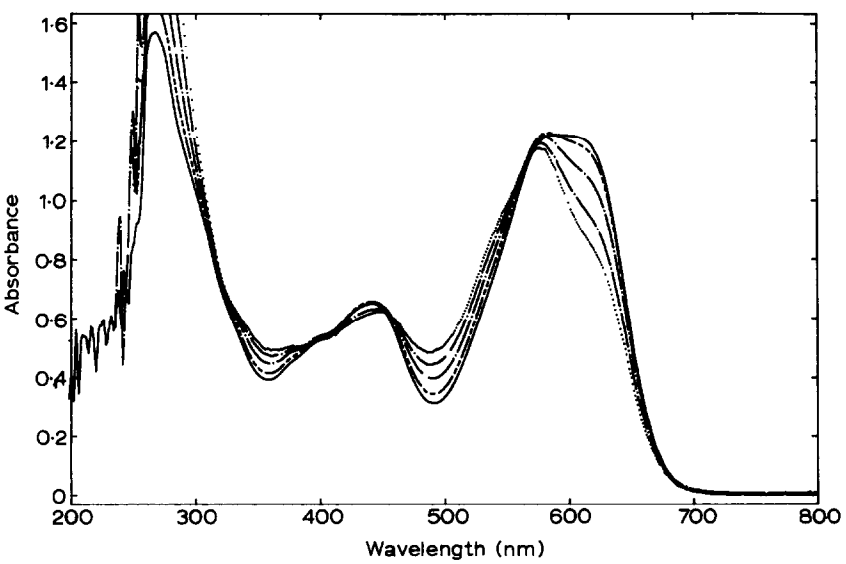

(b)

Fig. 2. (a) The normalized absorption spectra of **B** in DMF at $5{\cdot}05 \times 10^{-6}$ M (——); $1{\cdot}26 \times 10^{-6}$ M (– · –); $3{\cdot}16 \times 10^{-7}$ M (– –); $1{\cdot}58 \times 10^{-7}$ M (· · · · ·). (b) The normalized absorption spectra of **B** in DMSO at $5{\cdot}05 \times 10^{-6}$ M (——); $1{\cdot}26 \times 10^{-6}$ M (– – –); $6{\cdot}31 \times 10^{-7}$ M (– · –) $3{\cdot}16 \times 10^{-7}$ M (– · –); $1{\cdot}58 \times 10^{-7}$ M (· · · · ·). (The absorbance is given for the spectrum with the highest concentration in each case.)

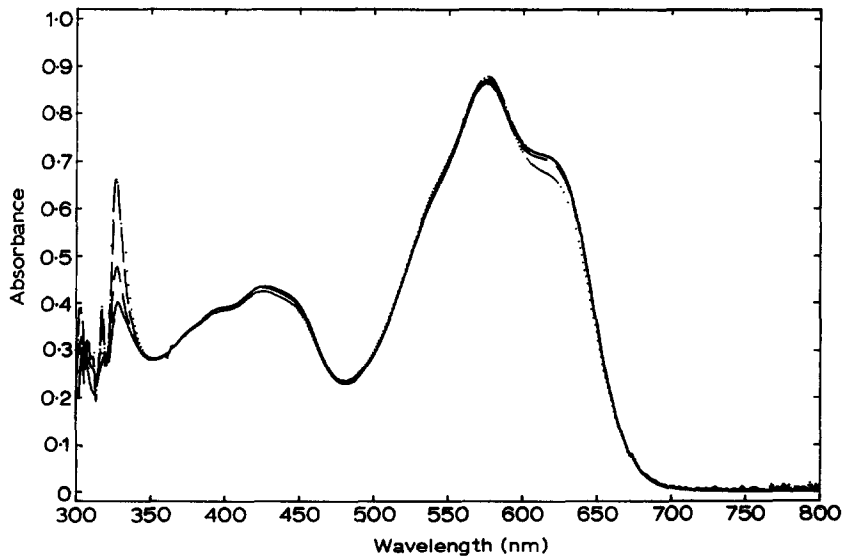

(a)

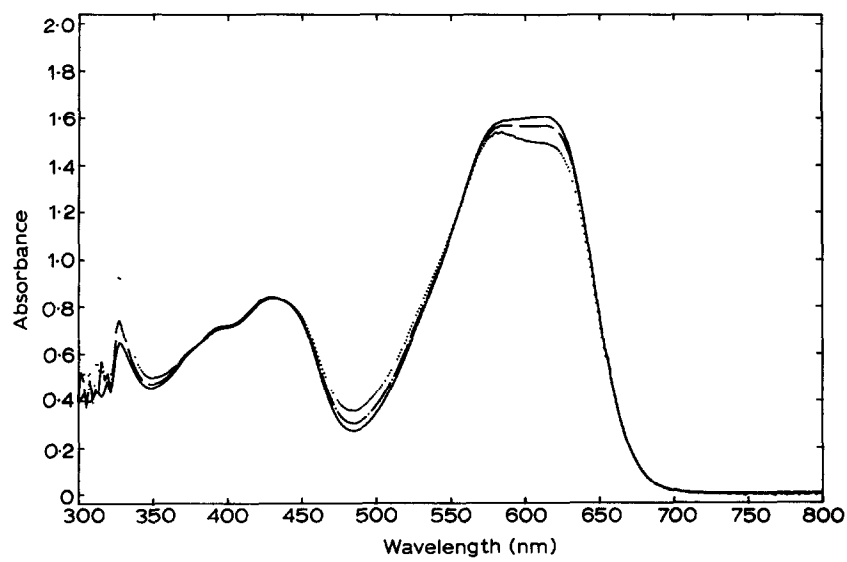

(b)

Fig. 3. (a) The normalized absorption spectra of **A** in acetone at $5{\cdot}28 \times 10^{-5}$ M (——); $2{\cdot}64 \times 10^{-5}$ M (– · –); $6{\cdot}61 \times 10^{-6}$ M (· · · · · ·). (b) The normalized absorption spectra of **B** in acetone at $5{\cdot}28 \times 10^{-5}$ M (——); $2{\cdot}64 \times 10^{-5}$ M (– · –); $1{\cdot}32 \times 10^{-5}$ M (· · · · · ·). (The absorbance is given for the spectrum with the highest concentration in each case.)

bands between 500 and 700 nm, while azo tautomers had them between 400 and 550 nm. There are three common features in these figures. First, the merging of the band at 450 nm with the higher wavelength absorption bands at diluted concentrations. Second, the absorption band above 600 nm decreases and the absorption band at about 550 nm increases as the concentrations of the dyes are reduced. The formation of isobestic points at about 320, 400 and 570 nm is also common, indicating the existence of a single aggregation equilibrium between dimer and monomer.[19]

The spectroscopic changes observed for **A** or **B** are opposite to those normally found for a clean monomer–dimer system in an aqueous solution, namely metachromatic changes. It was reported by Coates[20] that dyes having a delocalized charge as a part of the chromophoric system showed metachromatic disturbances with an increase in the high wavelength band and a decrease in the low wavelength band as the dye concentrations were reduced. The respective bands were inconclusively assigned to the monomer and dimer.[13] It was also reported that concentration dependent spectroscopic changes were minor for dyes without a delocalized charge. In contrast to Coates' results, **A** and **B** have the same spectroscopic changes, even though **B** is ionized whilst **A** is not.

The concentration dependent spectroscopic changes for **A** and **B** in acetone are not as striking as the corresponding changes in DMF or DMSO (Fig. 3(a) and (b)), suggesting little disturbance on the dye aggregates, which may remain strongly self-associated in acetone at very diluted concentrations. This is reasonable, because acetone is not as polar as DMF and DMSO and apparently does not break-up the dye aggregates.

3.2 Analyses of absorption profiles and calculation of λ_{max}

A more detailed understanding of the spectroscopic behavior of the dyes could be obtained from the curve analyses of representative absorption profiles and PPP-CI calculations of λ_{max} for various possible tautomers. The absorption profiles of **A** at 6·61 and $3{\cdot}30 \times 10^{-7}$ M (see Fig. 1(a)) and those of **B** at 6·61 and $1{\cdot}65 \times 10^{-7}$ M (see Fig. 2(a)) were chosen. In either system, there was a color transition from light blue to light pink at the lower concentrations. Each curve was broken up into eight Gaussian peaks by a nonlinear least square regression. Although excellent fits were achieved in all cases, as shown in Figs 4 and 5, we are aware of the uncertainties associated with the deconvolution of such complex absorption profiles, especially at the solvent cut-off regions (200–300 nm). An additional complication was encountered in the analyses of the solid state absorption curves (Fig. 6). Unlike the solution spectra, which showed zero absorbance above 700 nm, the solid state spectra of **A** and **B** in KBr showed descending tails that did not

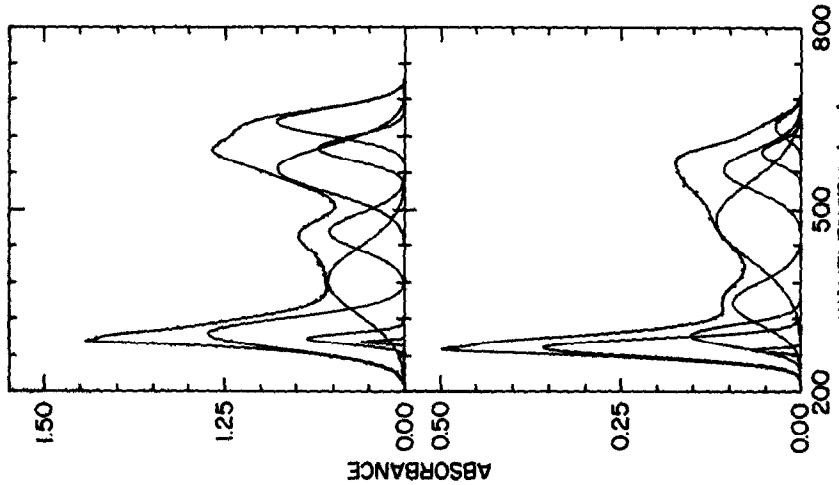

Fig. 5. The deconvoluted absorption profile for the spectra of **B** in DMF at (a) $6{\cdot}61 \times 10^{-7}$ M (top) and (b) $1{\cdot}65 \times 10^{-7}$ M (bottom).

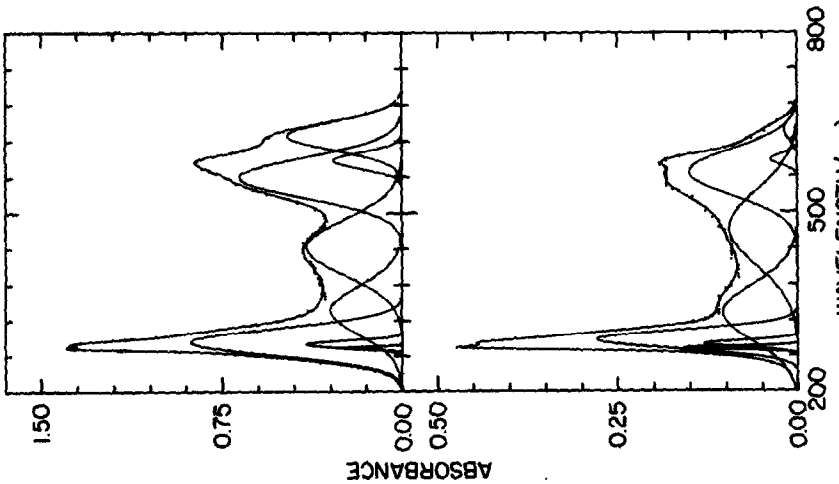

Fig. 4. The deconvoluted absorption profile for the spectra of **A** in DMF at (a) $6{\cdot}61 \times 10^{-7}$ M (top) and (b) $3{\cdot}30 \times 10^{-7}$ M (bottom).

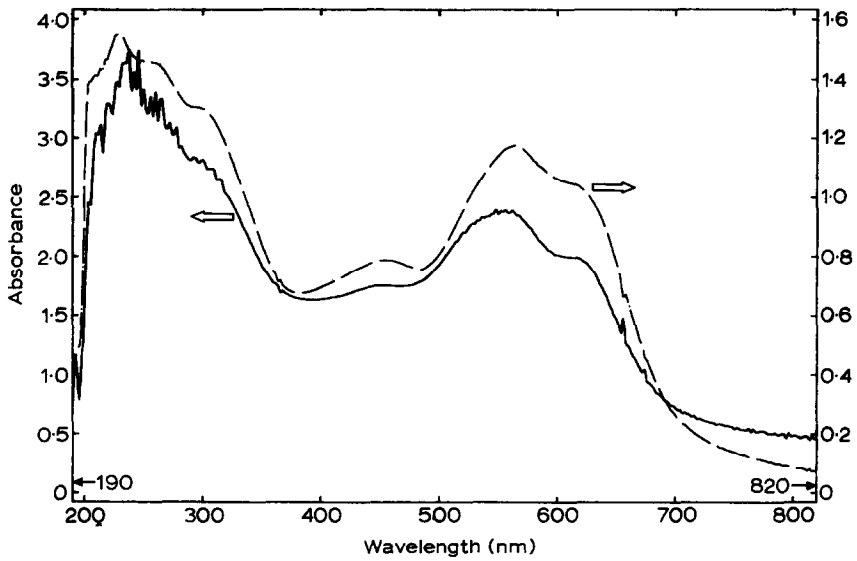

Fig. 6. The absorption spectra of **A** (——) and **B** (– · –) in KBr.

level off completely. In order to verify the reliability of the curve analyses, we decided to analyze each curve twice based on two assumed baselines. One of the baselines intersected the absorption curves at 700 nm and the other at 800 cm. We thought that the first baseline was reasonable because all the solution spectra zero at about 700 nm. The deconvoluted solid state spectra are shown in Figs 7 and 8.

The positions and the areas of the deconvoluted peaks for the solution and the solid state spectra are listed in Tables 2 and 3. Peaks at absorption wavelengths lower than 400 nm are not included. As shown in Table 2, peak 1 of the solution spectrum of **A** or **B** shifts to a higher wavelength with an

TABLE 2
Deconvoluted Peak Positions and Areas for the Solution Spectra of **A** and **B**

	A[a]		**A**[a]		**B**[b]		**B**[b]	
	λ_{max} (*nm*)	*Area %*	λ_{max} (*nm*)	*Area %*	λ_{max} (*nm*)	*Area %*	λ_{max} (*nm*)	*Area %*
Peak 1	438	33	467	47	447	19	474	59
Peak 2	553	40	560	47	550	42	557	28
Peak 3	581	7	582	3	584	15	586	8
Peak 4	622	20	631	3	626	24	627	5

[a] See Fig. 4(a).
[b] See Fig. 5(a).

TABLE 3
Deconvoluted Peak Positions and Areas for the Solid State Spectra of **A** and **B**

	A800[a]		**A700**[a]		**B800**[b]		**B700**[b]	
	λ_{max} (*nm*)	*Area %*	λ_{max} (*nm*)	*Area %*	λ_{max} (*nm*)	*Area %*	λ_{max} (*nm*)	*Area %*
Peak 1	446	37	451	34	443	48	445	46
Peak 2	560	32	552	30	560	29	552	27
Peak 3	629	11	591	12	632	8	588	10
Peak 4	631	20	633	23	636	15	634	17

[a] See Fig. 7(a).
[b] See Fig. 8(a).

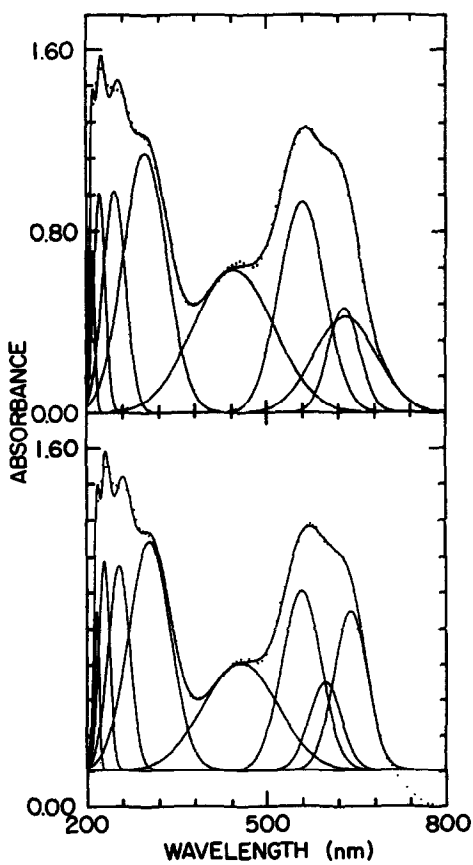

Fig. 7. The deconvoluted absorption profile for the spectra of **A** in KBr with the base line intersects the absorption curve at 800 nm (a, top) or 700 nm (b, bottom).

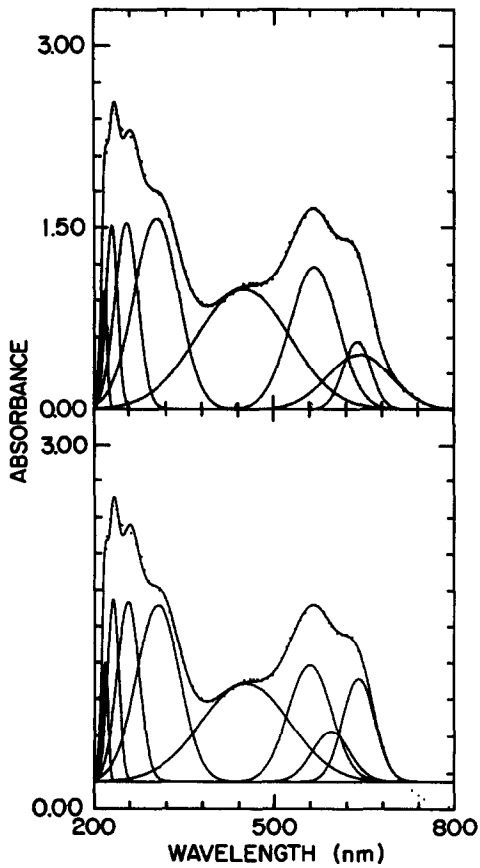

Fig. 8. The deconvoluted absorption profile for the spectra of **B** in KBr with the base line intersects the absorption curve at 800 nm (a, top) or 700 nm (b, bottom).

increase in its area at the diluted concentration, while peaks 2–4 show unchanged peak positions. The respective solid state data based on the 700 and 800 nm lines are similar (Table 3), except for the blue shift of peak 3 from about 630 to 590 nm. A good agreement for all the peak positions at approximately 450, 550, 580 and 630 nm for the solid state spectra (based on the 700 nm baseline) and for the solution spectra of **A** and **B** is realised.

To enable the peak assignment, PPP-CI calculations of λ_{max} and oscillator strengths (OS) for various possible tautomer structures were performed. There are two types of tautomers, namely neutral (**N1**–**N3**) and mono-ionic (**M1**–**M3**), as shown in Schemes 5 and 6 respectively, including the resonance form(s) for each tautomer. The di-anionic structures (**D1**–**D3**) shown in Scheme 7 are in resonance and can thus be expressed by a totally delocalized structure **D**, which is related to tautomer **IX** shown in Scheme 3, as discussed in Section 1. The partial charges on the oxygen and nitrogen atoms were an

average over the three di-ionic tautomers **D1, D2** and **D3**. Planar structures such as those shown in Scheme 4 were assumed for all the tautomers in the calculation. This assumption is highly probable because similar planar structures have been observed for several 4-(phenylazo)-3-hydroxy-naphthanilides, such as CI Pigment Red 2 and chloro derivatives of CI Pigment Brown 1 and CI Pigment Red 9.[21] In addition, the calculated values remained relatively unchanged by assuming a free rotating anilide group. The calculated λ_{max} and OS for the tautomers and several resonance structures (**N3**[7], **D1–D3** and **D**) are listed in Table 1. It is interesting to note that resonance forms **D1, D2. D3** and **D** show different λ_{max} and OS values, although the assumption of a fully delocalized charge was made for the calculation.

A reasonable peak assignment can readily be made for the deconvoluted

TABLE 4
Peak Assignments for IR and Raman Spectra (Values Given in cm^{-1})

A	B	Assignment
3 700–3 200	3 700–3 200	Bonded *trans* amide ν (N—H),
w, br	w, br	water ν (O—H)
3 098 w	3 111 w	Aromatic ν (C—H)
1 657 m	1 677 m	Amide ν (C=O)
1 603 s	1 600 s	Hydrazone ν (C=O), ν (>C=N) and ring ν (C=C)
1 609 m	**1 608 m**	Benzene ring ν (C=C)
1 550 s	1 553 s	ν as (o,p-NO_2)
1 553 s	**1 540 s**	
1 496 s	1 491 s	ν *cis* N=N)
1 491 s	**1 490 s**	
1 476 s	1 473 s shoulder	Not assigned
1 448 s	1 448 s	Not assigned
1 368 s	**1 370 s**	ν (trans N=N)
1 325 s	1 326 s	νs (NO_2)
1 350 s	**1 342 s**	
	1 312 s	νs (NO_2)
	1 310 m	
1 273 s	1 273 s	Azo ν (Ph—O) and hydrazone
1 284 s	**1 280 s**	ν (Ph—N)
1 238 m	**1 235 m**	Not assigned
1 209 w	1 207 w	Not assigned
1 177 s	1 177 s	ν (O—H) deformation
1 154 s	1 154 s	ν (Ph—N=)
1 160 s	**1 154 s**	

Definitions: w, weak; m, medium; s, strong; br, broad; md, medium doublet; sd, strong doublet.
Raman peak positions in bold.

spectra of **A** (in solution and in the solid state) by assigning **N1**, **N2** and **N3** to peaks 1, 2 and 3 respectively. Peak 4 may be due to various resonance forms of the tautomers. Accordingly, the increase in the area of peak 1 upon dilution indicates an increase in the percentage of the azo tautomer **N1**.

Although a straight forward peak assignment cannot be made for the deconvoluted spectra of **B**, rationalization of the spectra of **B** can still be made through the calculated λ_{max}. The absence of **M3** was indicated by the ^{1}H NMR spectrum of **B** showing a naphthoxy proton peak at 16·31 ppm (see Table 5). As shown in Table 1, tautomers **M1** and **M2** have the respective primary λ_{max} at 589 and 625 nm and the respective secondary λ_{max} at 419 and 438 nm. An overlapping of these λ_{max} values may give rise to the observed spectra of **B**, shown in Figs 2 and 6 with a major band at about 600 nm and a minor band at about 450 nm. Since the secondary λ_{max} of **M1** has a relatively high OS, an increase in its concentration will intensify the minor band. In this light we also arrived at a conclusion that the increase in the area of peak 1 upon dilution is due to an increase in the concentration of the azo tautomer **M1**.

3.3 Structural information from IR, Raman and NMR

The existence of azo tautomers for **A** and **B** was confirmed by IR and Raman, while ^{13}C NMR spectra suggested the existence of the hydrazone tautomers. The major absorption peaks of the IR and Raman spectra and the peak assignment are summarized in Table 4. The peak positions for **A**

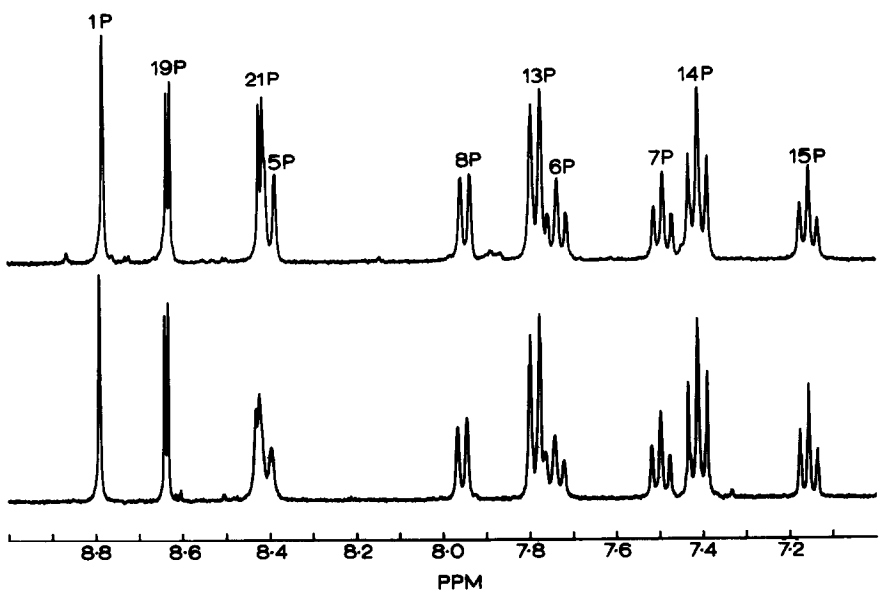

Fig. 9. ^{1}H NMR spectra for **A** (top) and **B** (bottom). The naphthol OH peaks at 16·30 PPM and the amide N–H peaks at 11·54 PPM not shown.

mimic the corresponding peaks for **B** except that the peak of the amide carbonyl for **A** absorbed at about 20 cm^{-1} lower than the corresponding peak for **B**, indicating an associated amide group in **A** and a free one in **B**.[22] In both cases, the Raman absorption bands at about 1490 and 1370 cm^{-1} are respectively attributed to the *cis* and *trans* N=N stretchings of the isomerizing azo tautomers.[3,23] The peak assignments were further substantiated by the fact that the *cis* N=N peak at 1490 cm^{-1} disappeared whilst the *trans* N=N peak remained as the strongest signal in the 1:2 chromium(III) or cobalt(III) complexes of **A**.

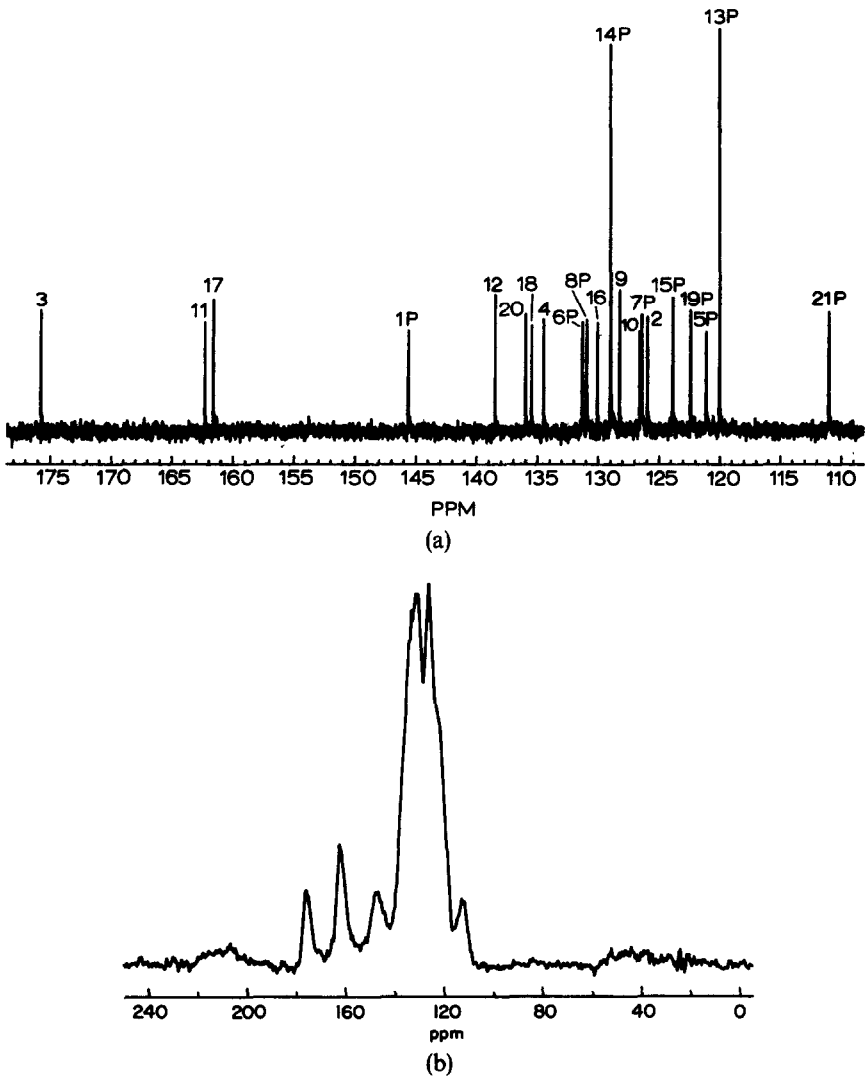

Fig. 10. ^{13}C NMR spectra for **A** (a) in DSMO and (b) in the solid state.

Compound **A** and **B** also showed essentially identical NMR results. The solution ^{1}H NMR spectra of **A** and **B** are shown in Fig. 9. Except for the slightly different peak shapes for the overlapped peaks at about 8·4 ppm, the chemical shifts for all the peaks were identical within the experimental error. This is unusual because deprotonation of phenols have been known to cause significant proton chemical shifts.[24,25] Identical ^{13}C NMR spectra were obtained for **A** and **B** in DMSO (Fig. 10(a)) as well as in the solid state (Fig. 10(b)). In each case, the furthest down field peak was at about 175·8 PPM, indicative of a ketone carbonyl carbon. This can only be accounted for with a naphthoquinone hydrazone tautomer **N2** and the peak is thus assigned to

TABLE 5
^{1}H NMR Peak Assignments for Naphthol AS and **A**[a]

	Picramic anid[b]	*Naphthol AS*	**A**
1p	—	8·50 (s, 1 H)	8·78 (s, 1 H
4(p)	—	7·34 (s, 1 H)	
5p	—	7·77 (d)	8·40 (d)
		J = 8·2 Hz	J = not clear
6p	—	7·53 (t, 1 H)	7·74 (t, 1 H)
		J = 7·6 Hz	J = 7·2 Hz
7p	—	7·38 (t, 1 H)	7·49 (t, 1 H)
		J = 7·6 Hz	J = 7·2 Hz
8p	—	7·94 (d, 1 H)	7·95 (d, 1 H)
		J = 8·1 Hz	J = 7·4 Hz
13p	—	7·77 (d, 2 H)	7·79 (d, 2 H)
		J = 8·2 Hz	J = 7·6 Hz
14p	—	7·43 (t, 2 H)	7·41 (t, 2 H)
		J = 7·6 Hz	J = 7·5 Hz
15p	—	7·16 (t, 1 H)	7·15 (t, 1 H)
		J = 7·6 Hz	J = 7·4 Hz
19p	8·22 (d, 1H)	—	8·63 (d, 1 H)
	J = 3·2 Hz		J = 3·1 Hz
21p	7·83 (d, 1 H)	—	8·42 (d, 1 H)
	J = 3·2 Hz		J = 3·1 Hz)
—N—H	—	10·63 (s, 1 H)	11·54 (s, 1 H)
—O—H (naphthyl)	—	11·35 (s, 1 H)	16·30 (s, 1 H)
—O—H (phenyl)	—	—	Not found[c]

[a] Definitions: s = singlet; d = doublet; t = triplet.
[b] See Ref. 26.
[c] This may be overlapped with the water peak or show up as a small side peak which was observed adjacent to the water peak.

the quinone carbonyl carbon (C–3). The peak position, which is very close to the chemical shift of 180 PPM known for pure naphthoquine hydrazones,[3,7] further suggests **N2** as the major tautomer. This is in agreement with the conclusion derived from UV-VIS that **N2** was the dominant tautomer for aggregated dye molecules. The second down field peak, visible in both the solution and the solid state spectra, at about 162·3 PPM is due to the amide carbonyl carbon. The third down field peak at 161·8 PPM of the solution spectrum indicates the presence of another carbonyl carbon and suggests the presence of a benzoquinone hydrazone tautomer **N3**. The peak is thus assigned to the phenoxy carbon (C–17). Complete peak assignments for the ^{1}H and ^{13}C NMR spectra for **A**, **B** and related compounds are given in Tables 5 and 6 respectively, based on a comparison with literature data on

TABLE 6
^{13}C NMR Peak Assignments for Relavent Compounds

Carbon number[a]	*Picramic acid*[b]	*Naphthol AS*[b]	*Model compound*[c]	**A**	**B**
1p		130·55	140·0 (135·8)	145·55	145·57
2		121·75	125·1 (120·4)	125·96	125·90
3		153·87	172·7 (155·8)	175·83	175·69
4(p)		110·61	132·8 (131·1)	134·46	134·46
5p		125·79	121·1 (120·3)	121·13	121·07
6p		128·14	128·2 (128·7)	131·42	131·29
7p		123·74	125·7 (124·8)	126·50	126·39
8p		128·74	128·9 (128·7)	131·00	130·91
9		126·88	129·6 (128·3)	128·00	128·19
10		135·82	127·5 (127·8)	126·58	126·58
11		165·69	—	162·27	162·26
12		138·50	—	138·37	138·43
13p		120·55	—	119·90	119·96
14p		128·82	—	128·98	128·94
15p		124·07	—	123·85	123·82
16	140·1		(134·4)	130·24)	130·04
17	146·4		(152·4)	161·70	161·60
18	133·1		(118·4)	135·65	135·48
19p	111·0		(132·0)	122·36	122·35
20	139·5		(120·3)	135·92	135·95
21p	107·5		(129·2)	110·97	110·97

[a] Protonated carbons are marked with a p.

[b] The peak assignment for ^{13}C NMR spectra of picramic acid and naphthol AS were found in the FIZ database provided by STN (Scientific and Technical Information Network) International from BASF Aktiengesellschaft. The assignment for **5p** and **6p** were corrected based on the corresponding ^{1}H–^{13}C 2D spectrum.

[c] Reported peak assignment for 1-(2′-hydroxyphenylazo)-2-naphthol in DMSO-d_6 or $CDCl_3$ (in parentheses) given in Refs 10 and 11.

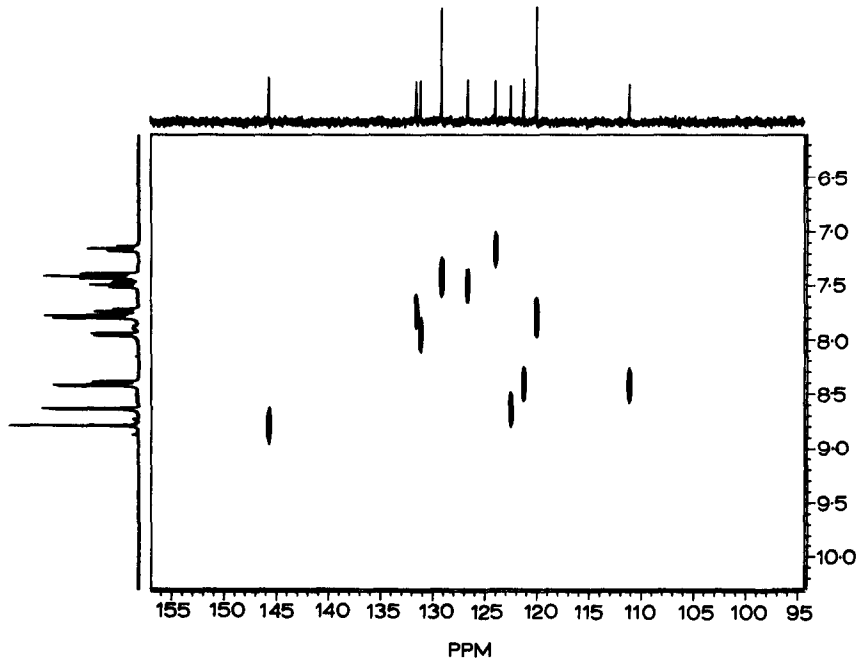

Fig. 11. ^{1}H–^{13}C correlated 2-D NMR spectra for A in DMSO.

related structures and ^{1}H-^{13}C 2D NMR spectrum such as that shown in Fig. 11. (It is interesting to note from the ^{13}C NMR data of 1-(2'-hydroxyphenylazo)-2-naphthol (Table 6) that the corresponding naphthoquinone hydrazone is the major tautomer in DMSO, and there exists only an azo tautomer in chloroform.[10,11])

3.4 A possible mechanism for the tautomerism

The surprising fact that **A** and **B** showed almost identical UV-VIS, IR, Raman and NMR spectra suggests that there may be a common intermediate for the tautomers of **A** or **B**. This intermediate could well be **Q** (Scheme 8) which has a completely delocalized planar ring structure and may be regarded as di-anionic with two protons or one proton and one sodium ion as the counter ions. Also, the protons and the sodium atom may undergo rapid intramolecular switching between the oxygen and the nitrogen atoms, similar to that reported for 1-(phenylazo)-2-naphthols,[7] and a neutral dye such as **A** could be as ionic as a deprotonated counterpart **B**. As a result, **A** and **B** may have an identical electronic structure and thus showed essentially identical spectroscopic results. In addition, **Q** may be the transitional species linking the other three tautomers (**N1**, **N2** and **N3**, Scheme 8) and is observed

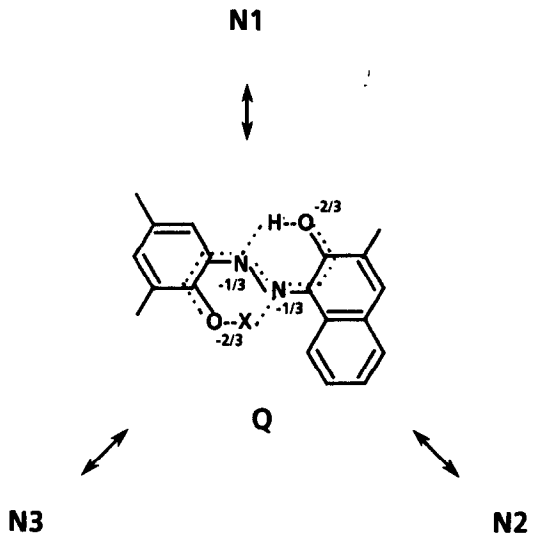

X = H or Na

Scheme 8

by UV-VIS (peak 4) and by NMR where the time scale does not permit the observation of the individual tautomers.

4 CONCLUSIONS

Isobestic points were found for the concentration dependent UV-VIS spectra (in DMF or DMSO) of azo dye **A** and its sodium salt **B** indicative of a dimer–monomer equilibrium for the dye molecules. Selected UV-VIS absorption profiles were deconvoluted into individual Gaussian peaks. Peak assignment was made by matching the peak positions and the calculated λ_{max} of several possible tautomers. This led to the conclusion that the concentration dependent spectroscopic shifts were due to the shifting of the hydrazone–azo equilibrium, which in turn was caused by a shift of the dimer–monomer equilibria. Specifically, hydrazone tautomers dominated in the dimeric or aggregated state while azo tautomers prevailed in very diluted solutions where most of the dye molecules were in monomeric form. The existence of the various tautomers were further confirmed by IR, Raman and NMR. We were intrigued by the fact that **A** and **B** showed almost identical spectroscopic results from IR, Raman and NMR. To account for this, a common intermediate involving a dianionic species was proposed for the tuatomerism of **A** and **B**. This type of intermediate may be common for *o,o'*-dihydroxy azo dyes.

REFERENCES

1. Haessner, R., Mustroph, H. & Borsdorf, R., *Dyes and Pigments*, **6** (1985) 277.
2. Kelemen, J., Moss, S. & Glitsch, S., *Dyes and Pigments*, **5** (1984) 83.
3. Kelemen, J., Moss, S., Sauter, H. & Winkler, T., *Dyes and Pigments*, **3** (1982) 27.
4. Ball, P. & Nicholls, C. H., *Dyes and Pigments*, **3** (1982) 5.
5. Zaitsev, B. E., Sycheva, E. D., Sheban, G. V., Lisitsyna, E. S., Mikhailova, T. A., Rodionova, G. N. & Dyumaev, K. M., *Zh. Org. Chim.*, **23** (1987) 1743.
6. Bershtein, I. Ya. & Ginzburg, O., *Russ. Chem. Revs.*, **23** (1972) 97.
7. Olivieri, A. C., Wilson, R. B., Paul, I. C. & Curtin, D. Y., *J. Am. Chem. Soc.*, **111** (1989) 5525.
8. Yagi, Y., *Bull. Chem. Soc. Jpn*, **47** (1964) 1875.
9. Pilipenko, A. T. & Savranskii, L. I., *Zh. Prikl. Spektr.*, **13** (1970) 918.
10. Fedkory, L. A., Zhukov, M. S. & Ermakov, A. N., *Izv. Akad. Nauk., SSSR Ser. Khim.*, **5** (1984) 1185.
11. Fedorov, L. A., Zhukov, M. S., Korsakova, N. V., Dedkov, Yu. M. & Ermakov, A. N., *Izv. Akad. Nauk., SSSR Ser. Khim.*, **8** (1983) 1763.
12. Dedkov, Yu. M. & Kotov, A. V., *Izv. Akad. Nauk., SSSR Ser. Khim*, **6** (1971) 1334.
13. Burdett, B. C. in *Aggregation Processes in Solution. Studies in Physical and Theoretical Chemistry, Vol. 26*, ed. E. Wyn-Jones & J. Gormally. Elsevier, New York, 1983, p. 259.
14. Fabian, J. & Hartmann, H. In *Light Absorption of Organic Colorants*. Springer-Verlag, Berlin, 1980, p. 72.
15. Bax, A. & Morris, G., *J. Magn. Res.*, **42** (1981) 501.
16. Griffiths, J., *Dyes and Pigments*, **3** (1982) 211.
17. Niimura, I., Imagome, H., Yamaga, H., Akuzawa, N., Yuta, K. & Kurahashi, T., US Patent 4,433,040, 1984.
18. Hsieh, B. R., *Dyes and Pigments*, in press.
19. Hamada, K., Kubota, H., Ichimura, A., Iijima, T. & Amiya, S., *Ber. Bunsenges. Phys. Chem.*, **89** (1985) 859.
20. Coates, E. J., *J. Soc. Dyers and Colourists*, **85** (1969) 355.
21. Whitaker, A., *Ibid.*, **94** (1978) 431.
22. Nakanishi, K. & Solomon, P. H. In *Infrared Absorption Spectroscopy*. Holden-Day, Inc., Oakland, 1977, p. 42.
23. Connor, J. A., Fine, D. J. & Price, R., *J. Chem. Soc. Dalton Trans.*, **89** (1981) 559.
24. Ewing, D. F., *Org. Magn. Reson.*, **12** (1979) 499.
25. Maciel, G. E. & Natterstad, J. J., *J. Chem. Phys.*, **42** (1965) 2427.
26. Asahi Research Center Co. Ltd, *Handbook of Proton–NMR Spectra and Data. Volume 2*. Academic Press, New York, 1985, spectrum no. 814.